Delft University of Technology

Delft Center for Systems and Control

Technical report 18-029

Distributed constraint optimization for autonomous multi AUV mine counter-measures*

J. Fransman, J. Sijs, H. Dol, E. Theunissen, and B. De Schutter

If you want to cite this report, please use the following reference instead:
J. Fransman, J. Sijs, H. Dol, E. Theunissen, and B. De Schutter, "Distributed constraint optimization for autonomous multi AUV mine counter-measures," *Proceedings of the OCEANS 2018 Charleston*, Charleston, South Carolina, 7 pp., Oct. 2018. doi:10.1109/OCEANS.2018.8604924

Delft Center for Systems and Control
Delft University of Technology
Mekelweg 2, 2628 CD Delft
The Netherlands
phone: +31-15-278.24.73 (secretary)
URL: https://www.dcsc.tudelft.nl

* This report can also be downloaded via https://pub.bartdeschutter.org/abs/18_029.html

Distributed constraint optimization for autonomous multi AUV mine counter-measures

Jeroen Fransman[a], Joris Sijs[a], Henry Dol[b], Erik Theunissen[c], Bart De Schutter[a]

***Abstract*— In this paper, Mine Counter-Measures (MCM) operations with multiple cooperative Autonomous Underwater Vehicles (AUVs) are examined within the Distributed Constraint optimization Problem (DCOP) framework. The goal of an MCM-operation is to search for mines and mine-like objects within a predetermined area so that ships can pass the area through a safe transit corridor. Performance metrics, such as the expected time of completion and the level of confidence that all mine-like objects within the area have been detected, are used to quantify the utility of the operation. The AUVs coordinate their individual search segments in a distributed manner in order to maximize the global utility. The segmentation is optimized by the Compression-DPOP (C-DPOP) algorithm, which allows explicit reasoning by the AUVs about their actions based on the performance metrics. After initial segmentation of the mine threat area, subsequent optimizations are triggered by the AUVs based on the variations in sonar performance. The performance of the C-DPOP algorithm is compared to a static segmentation approach and validated using the high-fidelity Unmanned Underwater Vehicle (UUV) simulation environment based on the Gazebo simulator.**

***Index Terms*— AUV, DCOP, C-DPOP, Gazebo, UUV-simulator, underwater search, mine counter-measures, MCM**

I. INTRODUCTION

The operational objective of a naval mine mission is a reduction of the risk that ships hit a mine while transiting through a particular body of water. Such risk reduction is achieved by conducting a Mine Counter-Measures (MCM) operation. An overview of a multi Autonomous Underwater Vehicle (AUV) MCM operation can be seen in Figure 1.

As defined in [2], the MCM operation consists of several sub-tasks:

1) Detection: detect mine-like objects as mine-like echos (MILECs) by scanning the MCM area with a larger sonar range yet a lower resolution;
2) Classification: revisiting MILECs and scanning with a higher resolution yet lower sonar range to classify them as a mine-like contact (MILCO) or a false positive (NON MILCO);
3) Identification: revisiting MILCOs to acquire optical images that are assessed by a human operator to identify the MILCO as a mine or a false positive;

[a] Delft Center for Systems and Control, Delft University of Technology, Delft, The Netherlands, j.e.fransman@tudelft.nl
[b] Netherlands Organisation for Applied Scientific Research (TNO), The Hague, The Netherlands
[c] Netherlands Defence Academy (NLDA), Den Helder, The Netherlands
[1] Icons from the Noun Project by Eugene Dobrik, Dinosoft Labs, and Arif Fajar Yulianto.

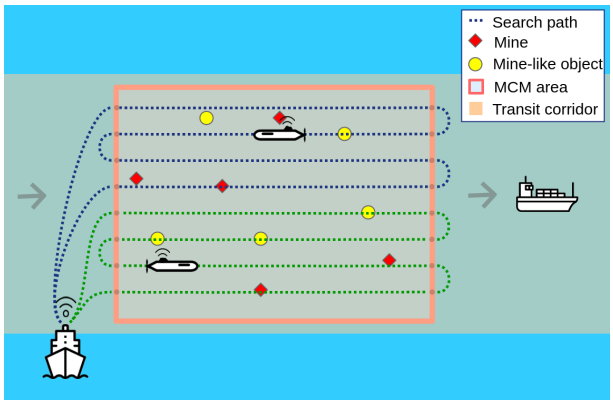

Fig. 1. An overview of a multiple Autonomous Underwater Vehicles (AUVs) Mine Counter-Measures (MCM) operation, adapted[1] from [1]. The goal is to clear the transit corridor for shipping traffic by detecting all mines within the operation area. The AUVs are launched from a support vessel and afterwards they traverse lawnmower search paths.

4) Disposal: revisiting all mines to perform disposal.

In this work, the focus is on the segmentation of the MCM area within the detection task for multiple cooperating AUVs. In the near future, the detection task will be performed by multiple AUVs in an autonomous manner [3]. The segmentation will be performed based on nominal sonar performance indicators such as the effective sonar range [4]. After the segments are scanned by the AUVs, the results are assessed at the support vessel [5]. In case of unsatisfactory results due to variations in the achieved sonar performance, the operation could be extended to cover the regions that are not adequately scanned [6]. This process increases the total operation time considerably. In order to reduce the required time, the search segments could be adapted during the operation through feedback from the AUVs.

There exists a wide range of related work involving adaptive search for both AUVs and Unmanned Surface Vessels (USVs). Most works focus on the coverage path planning problem in which a path needs to be optimally planned for a sensor to cover a certain area [7]. In the approach of [8], the search area is discretized based on "equal information gain" of the discrete segments. USVs are assigned to explore segments yielding the least amount of cost for the individual USVs. A similar approach is taken in [9] with multiple AUVs for optimal resource allocation based on motion costs, uncertainty reduction, and optimization over secondary objectives such as communication bandwidth and energy consumption. These approaches require the discretization of the search area. A common problem of discretization is the exponential

memory requirement when the total survey area increases [10]. This problem is alleviated in [11] and [12] through approximation and a dynamic programming [13] approach based on information gain. These centralized optimization approaches, where the support vessel optimizes the segmentation of all AUVs in-situ, are considered infeasible due to communication constraints on both range and bandwidth [14]. Communication between AUVs is considered viable, since during the operation their distance is not as extensive. Furthermore, the AUVs could form a communication network in which messages can be passed between AUVs that have no direct connection. However, a centralized approach, where an AUV receives all information and optimizes the actions of all AUVs, is considered impractical due to the low processing power of the AUVs.

For these reasons, in this work, the coverage path planning is modeled and solved in a distributed manner by the Compression-DPOP (C-DPOP) algorithm [15]. The distributed approach allows for in-situ adaption of the search segments through inter-AUV communication without discretization of the search area. The C-DPOP algorithm is applied to the MCM problem modeled within the Distributed Constraint Optimization Problem (DCOP) framework.

The remainder of this paper is outlined as follows. Section II defines the MCM detection task problem as a coverage path planning problem. Afterwards, the DCOP framework and the C-DPOP algorithm are detailed and the detection problem is modeled as a DCOP in Section III. In Section IV, the performance of the C-DPOP algorithm is compared to a static approach within a high fidelity simulation environment. Finally, the results are discussed in Section V.

II. PROBLEM STATEMENT

The detection task is based on two local performance metrics of the AUVs:

1) Expected time of Completion (EoC): expected time for completing the search segment of the agent;
2) Probability of Detection (PoD): the level of confidence that all mine-like objects within the segment have been detected as a mine-like echo (MILEC)

The task is completed when the PoD of the search area is higher than the required PoD (P^{req}) within a maximum operation time $t^{\max}$, which are both set by an operator.
The MCM search area is modeled as a monotone rectilinear polygon, $s = (x, y, w, h)$, where x, y indicate the center of the area and w, h denotes the width and height, respectively. The scan segment of AUV i is defined similarly to the MCM area as $s_i = (x_i, y_i, w_i, h_i)$. The combined segments of all AUVs is denoted as $S = \bigcup_{i=1,\dots,n} s_i$, where n is the number of AUVs. An example of segmentation for two and three AUVs can be seen in Figure 2. The total operation time defined as $T = \max_{i=1,\dots,n} T_i$, where T_i is the EoC of AUV i.

The AUVs are equipped with a pair of Side Scan Sonars (SSS) (mounted on the port and starboard side) in order to scan according to a *lawnmower* pattern. This pattern is optimal for rectangular search areas where the turn radius

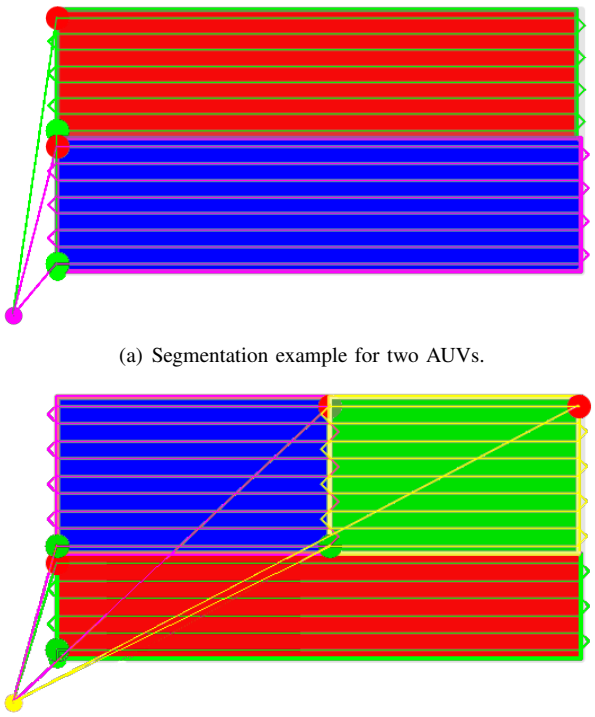

(a) Segmentation example for two AUVs.

(b) Segmentation example for three AUVs.

Fig. 2. Initial segmentation of an MCM search area. The covered segments of the AUVs are presented as colored areas. The lawnmower patterns of the AUVs are shown as contrasting colored lines starting from and finishing in a colored circle. These circles indicate the initial and rendezvous position, respectively. The green and red circles mark the start and finish of the lawnmower pattern.

of the AUV (d_i^{turn}) is smaller than the distance between the *legs*, which is determined by the sonar range (r_i) [16]. For AUVs the sonar range is typically several factors higher than the turn radius, therefore only lawnmower patterns are considered in this work.

The sonar range is defined as the distance over which the sonar achieves a particular PoD. It is based on the properties of the SSS, the environment, and the height over the seabed during scanning. Sailing close to the seabed results in a short sonar range and a high PoD since the Signal-to-Noise Ratio (SNR) of the sonar will be high. An increase in height will result in an increase of the sonar range, but consequently decreases the SNR and thereby the PoD. Based on this trade-off the height over the seabed is fixed during scanning based on the required PoD for the MCM search area. Additional AUV properties which are taken into account are the velocity during travel (v_i^{transit}), and the velocity during scanning (v_i^{scan}).

The EoC for agent i (T_i) is a function of the scan segment s_i and the transit time based on the initial position of the agent,

$$T_i = t_i^{\text{initial}} + t_i^{\text{scan}} + t_i^{\text{return}}$$

where t_i^{initial} is the initial transit time towards the scan segment, t_i^{scan} is the time spend scanning, and t_i^{return} is the rendezvous time from the scan segment back to the initial

position.

The transit times depend on the Euclidean distance $d(\cdot,\cdot)$ and the transit velocity of the AUV as,

$$t_i^{\text{initial}} = d(p_i^{\text{initial}}, p_i^{\text{start}})/v_i^{\text{transit}}$$
$$t_i^{\text{return}} = d(p_i^{\text{initial}}, p_i^{\text{finish}})/v_i^{\text{transit}}$$

where $p_i^{\text{initial}} = (x_i^{\text{initial}}, y_i^{\text{initial}})$, $p_i^{\text{start}} = (x_i^{\text{start}}, y_i^{\text{start}})$, and $p_i^{\text{finish}} = (x_i^{\text{finish}}, y_i^{\text{finish}})$ indicate the position of the initial location, start of the first leg, and the finish of the final leg, respectively. Note that, since the depth is considered as a constant, it is neglected from the notations.

The time spent scanning (t_i^{scan}) depends on the total length of the legs and the number of turns within the lawnmower pattern. In order to minimize the number of turns, the longest side of the scan segment ($d_i^{\text{long}} = \max(w_i, h_i)$) is taken as the scan direction of the agent. As a result, the shortest side ($d_i^{\text{short}} = \min(w_i, h_i)$) is used to determine the number of required legs l_i within the lawnmower pattern according to the sonar range of the agent. The size of the turns is determined by the turn radius of the AUV (d_i^{turn}) and the distance between the legs (d_i^{leg}). Consequently, the time spent scanning is defined as

$$t_i^{\text{scan}} = \frac{l_i d_i^{\text{long}}}{v_i^{\text{scan}}} + \frac{\left(2d_i^{\text{turn}} + d_i^{\text{leg}}\right)(l_i - 1)}{v_i^{\text{scan}}}$$
$$l_i = \left\lceil \frac{d_i^{\text{short}}}{2r_i} \right\rceil$$
$$d_i^{\text{leg}} = \frac{d_i^{\text{short}}}{l_i}$$

where $\lceil\cdot\rceil$ denotes the ceiling function. Note that the number of legs l_i depends on the combined range of the two SSS systems of the AUV.

The global goal function G is defined as the utility relation between areas covered with sufficient PoD and the EoC, formalized as a rectangular Gaussian distribution,

$$G = \exp\left(-\left(\frac{(R^{\text{coverage}} - 1)^2}{(\sigma^{\text{coverage}})^2}\right)^{f^{\text{coverage}}} - \left(\frac{(R^{\text{time}})^2}{(\sigma^{\text{time}})^2}\right)^{f^{\text{time}}}\right)$$

$$R^{\text{coverage}} = \lambda(S)/\lambda(s), \qquad R^{\text{time}} = T/t^{\max}$$

where $\lambda(\cdot)$ denotes the Lebesgue measure [17] indicating the area of a segment, R^{coverage} is the ratio of the MCM area that is covered to the required PoD, R^{time} is the time ratio of the required time over the maximum allowed time $t^{\max}$. An operator can tune the relative significance between coverage and required time through the scale factors σ^{coverage}, σ^{time}, f^{coverage}, and f^{time}. Using these factors, the relative importance can be indicated between the coverage and time ratio, as well as the slopes of the utility function with respect to coverage and required time. A graphical overview of the global utility is depicted in Figure 3.

The global goal function, as described above, is iteratively optimized throughout the detection operation. After the initial optimization, the AUVs start to traverse their lawnmower patterns and, after every leg, their achieved sonar range is assessed. Due to seabed conditions and environmental conditions such as current, the achieved sonar range could deviate from their nominal sonar range. If an AUV detects a variation from the nominal sonar range r_i, it sends a trigger to all AUVs to reinitialize the optimization. If there is no variation, it will continue to traverse the remaining legs without informing the other AUVs. This decreases the required level of communication, which is beneficial for communication-constrained underwater search operations.

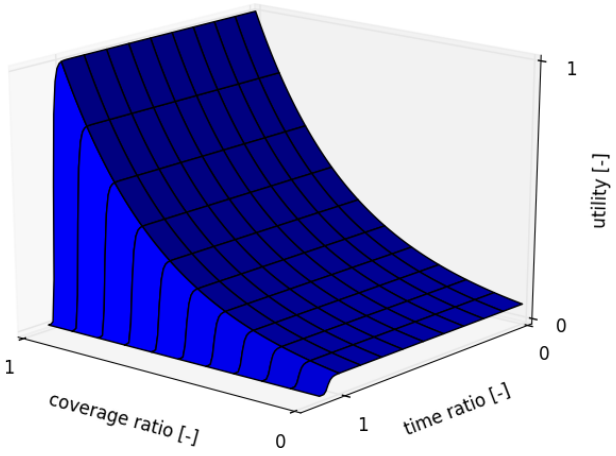

Fig. 3. An overview of the global utility function that is based on the ratio of the area of the covered segment R^{coverage} and the required time ratio R^{time} with $\sigma^{\text{coverage}} = 0.25$, $\sigma^{\text{time}} = 0.75$, $f^{\text{coverage}} = 0.5$, and $f^{\text{time}} = 50$. Note the steep drop at time ratio equal to 1, indicating that (almost) no utility is gained when the required time exceeds the maximum available time.

When the optimization is triggered, the remaining MCM area is updated by subtracting the segments that have been sufficiently covered. After the solution is found, the AUVs resume their search based on the updated solution. This process is repeated every time an AUV triggers the optimization.

III. DISTRIBUTED CONSTRAINT OPTIMIZATION PROBLEM

In this work, the MCM detection operation is modeled as a Distributed Constraint Optimization Problem (DCOP), which is a generalization of a Distributed Constraint Satisfaction Problem (DCSP) [18].

A DCOP is defined by a tuple $< A, X, D, F, G >$ [19] where;

A	is a set of agents
X	is a set of decision variables
D	is a set of domains for all variables
F	is a set of utility functions
G	is the global objective function

A DCOP is distributed in the sense that agents only interact with agents that are coupled through their variables by a utility function. This allows for the modeling of the problem as a constraint or function graph, thereby deconstructing the problem into an ordered pseudo-tree, making it possible to optimize various subproblems in parallel, such as the calculation of the EoC for all the AUVs within the MCM

detection task. The nodes of the graph represent the local actions of the AUVs while edges represent a constraint or utility relation between the actions. An example of a

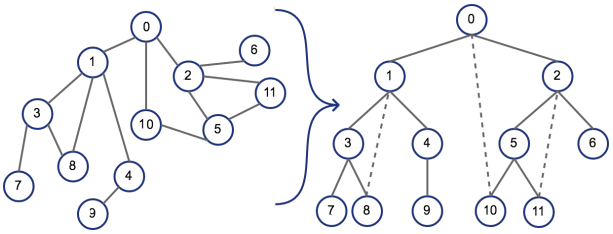

Fig. 4. An plot of the conversion of a DCOP problem as a constraint graph into a pseudo-tree. The nodes represent variables or actions that should be optimized. The edges represent a constraint or utility relation between the nodes. Indirect or pseudo-connections are illustrated as dotted edges.

conversion from a constraint graph into a pseudo-tree can be seen in Figure 4.

This deconstruction makes the DCOP framework especially suitable for modeling multi-AUV operations, because the global performance of the AUVs can be described by the interactions of their local actions. For example, the total scanned area is the union of all the segments scanned by the agents.

The goal of a DCOP is to optimize the global utility function by assigning values for all variables in a distributed manner. The complete allocation of all variables is denoted as $\mathfrak{X} = \bigcup_{i=1}^{n} X_i$. The variables can be assigned a value from within a bounded domain, denoted as the action space $\mathfrak{D} = \bigcup_{i=1}^{n} D_i$. Within the detection task, this indicates the allocation of segments to the AUVs within the MCM search area. AUVs coordinate their actions by exchanging messages about the utility of the interactions between their variables. The cost (in time) and benefit (in coverage) of the segmentation are expressed in terms of utility towards the global goal.

These variables are optimized *in situ* in collaboration with all other AUVs by the Compression-DPOP (C-DPOP) algorithm [15]. C-DPOP is based on the Distributed Pseudo-Tree Optimization Procedure (DPOP) [20], which is a DCOP solver that uses dynamic programming elements to communicate accumulated information about the global utility. DPOP requires a fixed number of communication steps during optimization, which is beneficial for MCM since underwater communication is subject to severe constraints.

A drawback is that the message size increases exponentially for large domains. This drawback is especially unfavorable for variables with continuous domains (D^{cont}) that are discretized to a high resolution, for example, the subdivision of the search area into a grid of predefined squares.

C-DPOP eliminates this drawback by iteratively creating discrete domains (D^{disc}) by sampling the continuous domains. At every iteration DPOP is applied to the discrete domains and the (local) optimum is used to compress the continuous domains around this optimum. The compression decreases the size of the continuous domains, which results

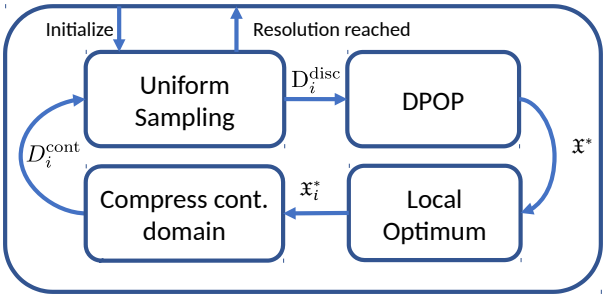

Fig. 5. An overview of the C-DCOP algorithm, where the discrete domains of AUV i, $D_i^{\text{disc}}(t)$ at time t are iteratively created from the continuous domains $D_i^{\text{cont}}(t)$. After the optimization the (locally) optimally assigned values of AUV i ($\mathfrak{X}_i^*$) are used to compress the continuous domains. The algorithm terminates when the resolution of all discrete domains is smaller than a predefined threshold.

in discrete domains of increasing resolution after every iteration. The algorithm terminates when the resolution of all discretized domains is smaller than a predefined threshold. An overview of the C-DPOP algorithm is given in Figure 5.

The MCM search operation is represented within the DCOP framework as

$$
\begin{aligned}
A &= (a_1, \ldots, a_n) \\
X &= (X_1, \ldots, X_n) \\
X_i &= \{s_i\} \\
D &= \left(D_1^{\text{cont}}, \ldots, D_n^{\text{cont}}\right) \\
D_i^{\text{cont}} &= \{s\} \\
F &= \{T_1, \ldots, T_n, \lambda(s_1), \ldots, \lambda(s_n)\} \\
G &= \exp\left(-\left(\frac{(R^{\text{coverage}}-1)^2}{(\sigma^{\text{coverage}})^2}\right)^{f^{\text{coverage}}} - \left(\frac{(R^{\text{time}})^2}{(\sigma^{\text{time}})^2}\right)^{f^{\text{time}}}\right)
\end{aligned}
$$

Note that the domains of the search segments are bounded by the MCM search area $s = (x, y, w, h)$.

IV. SIMULATION ENVIRONMENT

The performance of the C-DPOP algorithm for the MCM operations is validated through the high fidelity Unmanned Underwater Vehicle (UUV) simulation environment [21]. The simulator is based on the Gazebo simulator [22] and Robotic Operating System (ROS) [23] and includes hydrodynamic, (underwater) current, underwater sensor functions, and various AUV types. In this work, the AUVs are modeled after the A9-S of the ECA Group [24] as it is designed for seabed imagery. Figure 6 shows a rendering of the A9-S AUV as modeled within the UUV simulator [25].

Within the simulation environment, all AUVs are considered to be identical and therefore share all parameters such as maximum scan and transit velocities, sonar range, and turn radius. The parameters are chosen in accordance with the operational specification of the ECA A9 AUV [24].
The required PoD is set such that the sonar range is equal to 150 m, as defined within the specifications of the ECA A9. The maximum time is set corresponding to the time a single AUV would require to cover the entire MCM search area.

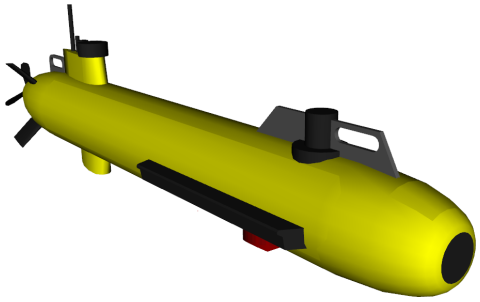

Fig. 6. A rendering of the A9-S AUV of the ECA Group [24] as modeled within the UUV simulator [25].

Two approaches are compared in order to assess the performance of the dynamic application of the C-DPOP algorithm. The first is a static approach in which the C-DPOP algorithm is executed once (at the start of the operation). The resulting segmentation is not updated during the operation. The second is a dynamic approach in which the segmentation is updated based on the triggers of the AUVs.

A. Simulation results

The performance of C-DPOP is assessed and compared to a static segmentation for multiple AUVs based on the nominal sonar performance. The performance is measured according to the global utility function based on the achieved covered area and required operation time. Two scenarios are evaluated in which the sonar range is less than nominal. The first scenario involves two AUVs, of which the sonar performance decreases gradually, and the MCM area covers 2 km $\times$ 1 km. The second scenario involves three AUVs, of which one has severely decreased sonar performance, and the MCM area covers 4 km $\times$ 4 km. In both scenarios the AUVs start at the rendezvous location to mimic the deployment by a support vessel.

In the first scenario, the reduction in sonar performance is not compensated within the static approach, which results in a loss of coverage over the entire width of the MCM area. By incorporating the feedback from the AUVs about the performance decrease, the search segments can be optimized within the dynamic approach based on the remaining available time to maximize the global utility.

Figure 7 shows the covered segments and trajectories of both approaches. The results in terms of the global utility, the time and coverage ratios are shown in Table I.

TABLE I

RESULTS OF THE FIRST SCENARIO.

Approach	time ratio	coverage ratio	global utility
Static	0.58	0.95	0.93
Dynamic	0.83	0.98	0.98

In the second scenario, similar results are achieved for the dynamic approach as the performance loss of one AUV is compensated by the others. In the static approach, the lack of additional optimization leaves large segments not covered, which increases the risk for undetected mines within that area. Figure 8 shows the final results for the static and dynamic approach in terms of the coverage segments and the trajectories of the AUVs. The results are summarized in Table II.

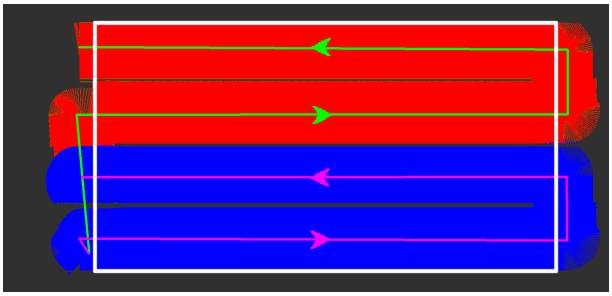

(a) Results of the static approach.

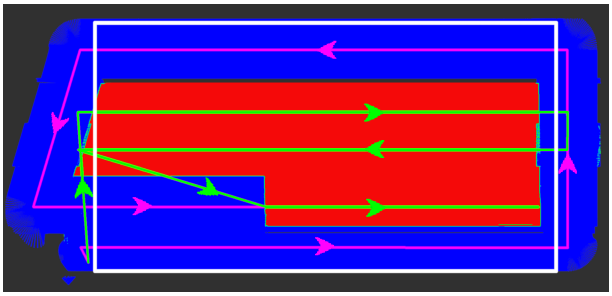

(b) Results of the dynamic C-DPOP algorithm.

Fig. 7. Example of the results for the first scenario of the static and dynamic C-DPOP algorithm. The MCM area is indicated by a white rectangle, the covered segments are color coded based on the individual AUVs. Within the segments, the lawnmower pattern is shown as lines with contrasting colors. As can be seen in (a), the static approach leaves several sections uncovered, while in (b) most of the area is covered by adjusting the search pattern. Note that during turns the scanned areas are incomplete, indicating decreased probability of detection.

TABLE II

RESULTS OF THE SECOND SCENARIO.

Approach	time ratio	coverage ratio	global utility
Static	0.88	0.87	0.83
Dynamic	0.95	0.99	0.99

B. Discussion

In both scenarios, the dynamic C-DPOP approach achieves a higher global utility. The utility increase depends on the size of the sonar performance loss during operation and the maximum available time of the operation. When the performance loss is moderate as in the first scenario, only slight gains can be achieved. However, in the second scenario, considerable performance loss can be overcome when the maximum operational time allows for additional legs within the search segments. When the available remaining time is limited, this improvement is reduced, since no time is available for additional searches.

The results of the two scenarios can be extended towards larger MCM areas without additional computational resources since no discretization of the MCM area is required.

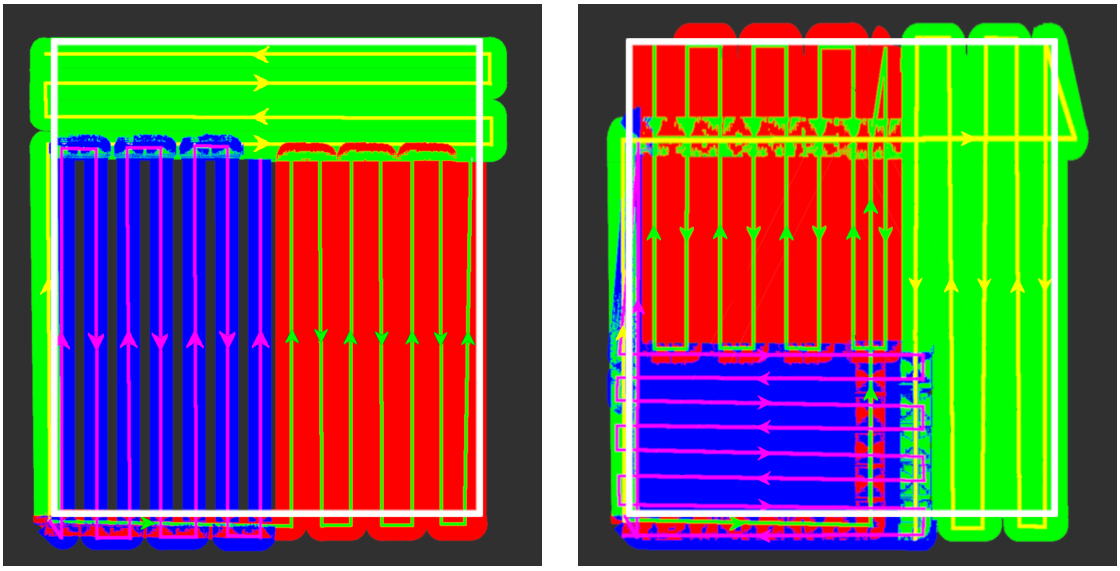

(a) Results of the static approach.

(b) Results of the dynamic C-DPOP algorithm.

Fig. 8. Example of the results for the second scenario of the static and dynamic C-DPOP algorithm. The MCM area is indicated by a white rectangle, the covered segments are color coded based on the individual AUVs. Within the segments, the lawnmower pattern is shown as lines with contrasting colors. As can be seen in (a), the sonar range of the AUV in the bottom left corner is severely decreased. In (b), the result of the dynamic optimization can be seen as the AUV decreases the distance between the legs and the other AUVs adjust their trajectories. Note that the dynamic approach covered several locations multiple times due to the change in orientation of the scan segments.

Furthermore, due to the assumption that the longest edge of the MCM area is used as scan direction, these results are analogous to MCM areas with other height to width ratios. For example, the segmentation for an MCM area of 2 km $\times$ 4 km is similar to the segmentation for an area of 4 km $\times$ 2 km. This assumption does not hold in practice for every height to width ratio, due to several aspects. Two of the most important aspects are the environmental properties and the positional uncertainty of the AUVs. Important environmental properties are underwater currents and bathymetry since both can severely deteriorate the sonar performance. Positional uncertainty is defined as the error between the actual and estimated position. The source of this uncertainty is due to the attenuation of Global Positioning System (GPS) signals underwater. AUVs are required to estimate their position during scanning instead of interpolating from the GPS signals. The estimation is typically performed through the use of inertial sensors, however, the position error for this estimation method is unbounded [26]. Therefore, the maximum leg length is often restricted based on the growth of the position error. In order to cope with this increasing error, the AUVs interrupt the scanning to acquire a GPS-fix by surfacing when the error crosses a (predefined) threshold.

V. Conclusions and Future Work

This paper presents a method to segment a search area of multiple cooperative Autonomous Underwater Vehicles (AUVs) in a distributed manner based on global performance metrics set by an operator. The application of the Distributed Constraint Optimization Problem (DCOP) framework is extended towards autonomous operations of multiple AUVs without the need for discretization of the Mine Counter-Measures (MCM) area, which allows for flexible modeling and optimization. The optimization of scan segments of the AUVs is initially performed based on nominal sonar performance and repeated when an AUV triggers a re-optimization during the operation. The performance of the C-DPOP algorithm is compared against static segmentation, which is the defacto standard for current multi-AUV operations. Results show higher achieved utility for the dynamic approach based on the Compression-DPOP (C-DPOP) algorithm.

Future work includes adding the position uncertainty of the AUVs during the operation as this results in significant operational limitations in practice [26]. Based on the position uncertainty the scanning trajectories can be adjusted such that the risk of collision between AUVs is minimized. Additionally, in order to reduce the position uncertainty the implementation of cooperative simultaneous localization and mapping (SLAM) [27] methods will be investigated.

References

[1] M. Cramer, "Understanding information uncertainty within the context of a net-centric data model: A mine warfare example," Tech. Rep., Mine Warfare Environmental Decision Aids Library (MEDAL), 2008.

[2] F. Florin, F. van Zeebroeck, I. Quidu, and N. Le Bouffant, "Classification performances of Mine Hunting Sonar: theory practical results and operational applications," *Undersea Defence Technology (UDT) Europe 2003*, Malmö, Sweden, June 2003.

[3] A. Belbachir, F. Ingrand, and S. Lacroix,"A cooperative architecture for target localization using multiple AUVs," *Intelligent Service Robotics*, vol. 5, no. 2, pp. 119–132, 2012.

[4] R. B. Wynn, V. A. I. Huvenne, T. P. L. Bas, B. J. Murton, D. P. Connelly, B. J. Bett, et al., "Autonomous Underwater Vehicles (AUVs): Their past present and future contributions to the advancement of marine geoscience," *Marine Geology*, vol. 352, pp. 451-468, 2014.

[5] E. Bovio, D. Cecchi, and F. Baralli, "Autonomous underwater vehicles for scientific and naval operations," *Annual Reviews in Control*, vol. 30, no. 2, pp. 117-130, 2006.

[6] D. P. Williams, F. Baralli, M. Micheli, and S. Vasoli, "Adaptive underwater sonar surveys in the presence of strong currents," *IEEE International Conference on Robotics and Automation*, pp. 2604-2611, June 2016.

[7] E. Galceran and M. Carreras, "A survey on coverage path planning for robotics," *Robotics and Autonomous Systems*, vol. 61, no. 12, pp. 1258-1276, 2013.

[8] B. Zhang, "Adaptive sampling with multiple mobile robots," *IEEE International Conference on Robotics and Automation*, 2008.

[9] D. Popa, A. Sanderson, R. Komerska, S. Mupparapu, D. Blidberg, and S. C. Chappel, "Adaptive sampling algorithms for multiple autonomous underwater vehicles," *IEEE/OES Autonomous Underwater Vehicles Conference*, pp. 108-118, 2004.

[10] K. H. Low, J. M. Dolan, and P. Khosla, "Adaptive multi-robot wide-area exploration and mapping," *Annual International Conference on Autonomous Agents and Multiagent Systems (AAMAS)*, pp. 23-30, 2008.

[11] K. H. Low, J. M. Dolan, and P. K. Khosla, "Information-theoretic approach to efficient adaptive path planning for mobile robotic environmental sensing,", *International Conference on Automated Planing and SCheduling (ICAPS)*, pp. 233-240, 2009.

[12] A. Meliou, A. Krause, C. Guestrin, and J. M. Hellerstein, "Nonmyopic informative path planning in spatio-temporal models," *National Conference on Artificial Intelligence (AAAI)*, pp. 602-607, 2007.

[13] R. Bellman, "Dynamic programming," Princeton University Press, 1957.

[14] S. Giodini, B. Binnerts, and K. Blom, "Can I communicate with my AUV?,"*Hydro International vol. Unmanned Systems*, pp. 24-27, 2016.

[15] J. Fransman, J. Sijs, H. S. Dol, E. Theunissen, and B. De Schutter, "Distributed constraint optimization for continuous mobile sensor coordination," in *European Control Conference*, (Limassol, Cyprus), 2018.

[16] V. Ablavsky and M. Snorrason, "Optimal search for a moving target: A geometric approach," in *AIAA Guidance, Navigation and Control Conference*, August 2000.

[17] H. Lebesgue, "Intégrale Longueur Aire," PhD thesis, Université de Paris, 1902.

[18] M. Yokoo, E. H. Durfee, T. Ishida, and K. Kuwabara, "The distributed constraint satisfaction problem: formalization and algorithms," *IEEE Transactions on Knowledge and Data Engineering*, vol. 10, no. 5, pp. 673–685, 1998.

[19] M. Pujol-Gonzalez, "Scaling DCOP algorithms for cooperative multi-agent coordination," PhD thesis, Universitat Autonoma de Barcelona, 2014.

[20] A. Petcu and B. Faltings, "DPOP: A Scalable Method for Multiagent Constraint Optimization," *IJCAI International Joint Conference on Artificial Intelligence*, pp. 266–271, 2005.

[21] M. M. M. Manhaes, S. A. Scherer, M. Voss, L. R. Douat, and T. Rauschenbach, "UUV simulator: A gazebo-based package for underwater intervention and multi-robot simulation", *OCEANS 2016 MTS/IEEE Monterey*, Sept. 2016.

[22] N. Koenig and A. Howard, "Design and use paradigms for gazebo, an open-source multi-robot simulator," *IEEE/RSJ International Conference on Intelligent Robots and Systems (IROS)*, pp. 2149–2154, 2004.

[23] M. Quigley, K. Conley, B. P. Gerkey, J. Faust, T. Foote, J. Leibs, R. Wheeler, and A. Y. Ng, "Ros: an open-source robot operating system," *ICRA Workshop on Open Source Software*, 2009.

[24] "ECA A9 AUV", 2018, [online] Available: `https://www.ecagroup.com/en/solutions/a9s-auv-autonomous-underwater-vehicle`

[25] "Model of the ECA A9 AUV", 2018, [online] Available: `https://github.com/uuvsimulator/eca_a9`

[26] L. Paull, S. Saeedi, M. Seto, and H. Li, "AUV navigation and localization: A review," *IEEE Journal of Oceanic Engineering*, vol. 39, no. 1, pp. 131–149, 2014.

[27] L. Paull, G. Huang, M. Seto, and J. J. Leonard, "Communication-constrained multi-AUV cooperative SLAM," *2015 IEEE International Conference on Robotics and Automation (ICRA)*, pp. 509-516, May 2015.